Taylor & Francis
Taylor & Francis Group

Natural Product Research
Formerly Natural Product Letters

ISSN: (Print) (Online) Journal homepage: https://www.tandfonline.com/loi/gnpl20

Glycosides from *Buddleja officinalis* with their protective effects on photoreceptor cells in light-damaged mouse retinas

Zehai Long, Xiaoye Du, Qiyao Wang, Zhijian Xu, Bo Li, Yong Zhang, Yu Chen, Qi Jia, Yiming Li & Weiliang Zhu

To cite this article: Zehai Long, Xiaoye Du, Qiyao Wang, Zhijian Xu, Bo Li, Yong Zhang, Yu Chen, Qi Jia, Yiming Li & Weiliang Zhu (2021): Glycosides from *Buddleja officinalis* with their protective effects on photoreceptor cells in light-damaged mouse retinas, Natural Product Research, DOI: 10.1080/14786419.2021.1944138

To link to this article: https://doi.org/10.1080/14786419.2021.1944138

NATURAL PRODUCT RESEARCH
https://doi.org/10.1080/14786419.2021.1944138

Glycosides from *Buddleja officinalis* with their protective effects on photoreceptor cells in light-damaged mouse retinas

Zehai Long[a], Xiaoye Du[b,c], Qiyao Wang[a], Zhijian Xu[d], Bo Li[d,e], Yong Zhang[d,e], Yu Chen[b,c,f], Qi Jia[a], Yiming Li[a] and Weiliang Zhu[d,e]

[a]School of Pharmacy, Shanghai University of Traditional Chinese Medicine, Shanghai, China; [b]Yueyang Hospital, Shanghai University of Traditional Chinese Medicine, Shanghai, China; [c]Clinical Research Institute of Integrative Medicine, Shanghai Academy of Traditional Chinese Medicine, Shanghai, China; [d]CAS Key Laboratory of Receptor Research; Drug Discovery and Design Centre, Shanghai Institute of Materia Medica, Chinese Academy of Sciences, Shanghai, China; [e]University of Chinese Academy of Sciences, Beijing, China; [f]Laboratory of Clinical and Molecular Pharmacology, Yueyang Hospital, Shanghai University of Traditional Chinese Medicine, Shanghai, China

ABSTRACT

A new phenylethanoid, hebitol IV (**1**), along with fifteen known glycosides (**2-16**), were isolated from water extract of the flower buds of *Buddleja officinalis*. Their structures were elucidated on the basis of 1 D-NMR, 2 D-NMR and MS data. Molecular docking showed the potential activities of the natural products against VEGFR-2. Bioassay results revealed that the compounds **10** and **14** exhibited strong inhibitory activity against VEGFR-2 with IC_{50} values of 0.51 and 0.32 μM, respectively. Moreover, the potential retinal protective effects of **10** and **14** were then investigated in the mouse model featuring bright light-induced retinal degeneration. The results demonstrated remarkable photoreceptor protective activities of **10** and **14** *in vivo*.

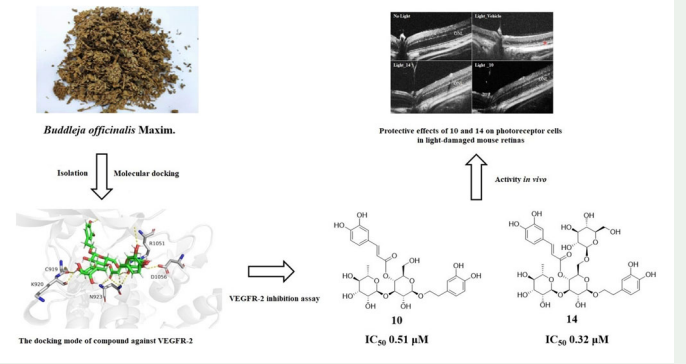

ARTICLE HISTORY

Received 19 April 2021
Accepted 8 June 2021

KEYWORDS

Loganiaceae; *Buddleja officinalis*; glycosides; VEGFR-2 inhibitory activity; photoreceptor protective activity

CONTACT Yong Zhang zhangyong109@simm.ac.cn; Qi Jia q_jia@126.com

Supplemental data for this article can be accessed online at https://doi.org/10.1080/14786419.2021.1944138.

1. Introduction

Retinal degenerative disease is a common and serious disease that causes blindness with high morbidity year by year, which is classified as "Shizhan Hunmiao" in Chinese and sudden blind by traditional Chinese medicine (TCM). Recent fact sheets (World Health Organization 2021) by the WHO (World Health Organization) indicated that at least 1 billion people have a preventable vision impairment globally. The research (American Macular Degeneration Foundation [date unknown]) on the pathological mechanism of retinal degenerative disease revealed that VEGF (vascular endothelial growth factor) signal pathway is one of the essential mechanisms on retinal neovascularization, closely related to the onset of retinal degenerative disease. And the VEGF receptor (VEGFR) inhibitor drugs have been used for treating retinal degenerative disease in clinical (Dugel et al. 2020).

Buddleja officinalis Maxim., belonging to the family Loganiaceae, is widely distributed in China (Editorial Committee of flora of China 1992), and its flower buds have been used as a traditional Chinese medicine for treating opacity of the cornea, photophobia, delacrimation, conjunctival congestion, and other eye diseases (Chinese Pharmacopoeia Commission 2020). Comprehensive phytochemical studies on *B. officinalis* revealed that more than 100 compounds have been isolated from this plant, including flavonoids (Matsuda et al. 1995), phenylethanoids (Zhang and Pan 1996), triterpene saponins (Guo et al. 2004), iridoids (Tai et al. 2011), monoterpene (Lee et al. 2013), lignans (Park et al. 2016) and alkaloids (Xie et al. 2019), which have shown several biological activities, such as anti-inflammatory (Tai et al. 2009), antiproliferative (Zhang and Pan 1996) and neuroprotective effect (Sheng et al. 2002). However, previous research on treatment of eye diseases of this plant mainly focused on the effect of extract (Jie and Gao 2004; Li et al. 2009; Shen et al. 2016), and no studies have been reported on compounds in this plant for the treatment of eye diseases. Furthermore, decoction boiled with water was the traditional usage of this herb to treat eye diseases. Herein, we report the isolation and structural elucidation of a new phenylethanoid, named hebitol IV (**1**), along with fifteen known glycosides (**2**-**16**) (Figure 1; Figure S1 in Supporting Information) from water extract of the flower buds of *B. officinalis,* as well as the evaluation of *in vitro* inhibitory activity of the sixteen

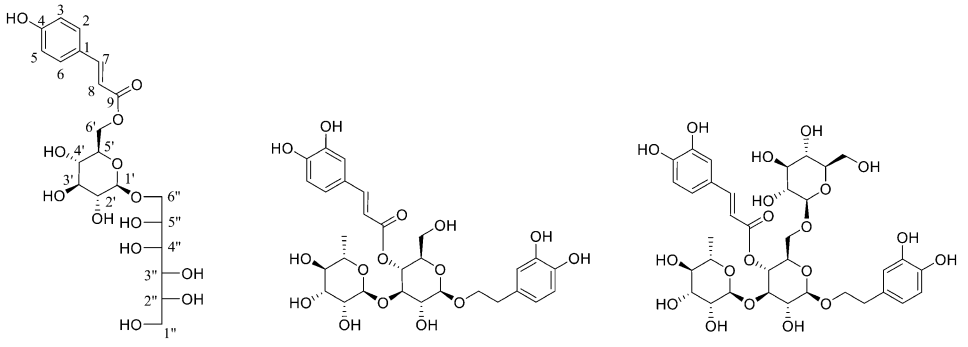

1 **10** **14**

Figure 1. Structures of compounds **1**, **10** and **14**.

compounds on VEGFR-2. Moreover, the potential retinal protective effects of **10** and **14** were then investigated in the mouse model featuring bright light-induced retinal degeneration.

2. Results and discussion

Compound **1** was obtained as a yellowish amorphous power. Its molecular formula was established as $C_{21}H_{30}O_{13}$ by HR-ESI-MS (*m/z*: 513.1584 $[M+Na]^+$). The IR spectrum showed absorption bands at 3355 cm^{-1}, 1695 cm^{-1}, 1630 cm^{-1},1603 and 1514 cm^{-1}, 1073 cm^{-1}, which suggested the existence of hydroxy, α, β-unsaturated ester carbonyl, olefinic, aromatic and ether functional groups, respectively. And the UV absorption bands at λ_{max} 225 and 310 nm also revealed the presence of aromatic rings. The ^1H NMR spectrum of **1** exhibited signals for AA′XX′ system at δ_H 7.47 (2H, d, $J=8.6$ Hz, H-2, 6) and 6.80 (2H, d, $J=8.6$ Hz, H-3, 5), *trans*-olefinic protons at δ_H 7.64 (1H, d, $J=15.9$ Hz, H-7) and 6.36 (1H, d, $J=15.9$ Hz, H-8), and sugar moieties at δ_H 3.27-4.52. The ^{13}C NMR spectrum revealed the presence of 21 carbon atoms, including a α, β-unsaturated ester carbonyl group at δ_C 169.1 (C-9), 146.9 (C-7), and 114.9 (C-8), six aromatic carbons at δ_C 161.4 (C-4), 131.3 (C-2, 6), 127.1 (C-1), and 116.8 (C-3, 5), and twelve carbons attributable to a sugar moiety (δ_C 64.6-105.0) and a hexitol moiety (δ_C 65.2-73.7). The carbon signals of α, β-unsaturated ester carbonyl group, along with the signal of *trans*-double bond and the AA′XX′ system suggested the presence of p-hydroxycinnamoyl group. The sugar moiety was deduced as glucopyranoside unit based on the six carbon signals (δ_C 105.0, 77.7, 75.6, 75.2, 71.6, and 64.6) and the corresponding proton signals (δ_H 3.27-4.52). In addition, the moiety acylated in the C-6′ position of glucopyranoside unit was deduced due to the downfield shift of C-6′ (δ_C 64.6). The left six carbon signals (δ_C 65.2-73.7) with the lack of an anomeric carbon signal (around δ_C 100) were assigned to a hexytol moiety, which was determined as mannitol based on the coincidence of the corresponding carbon atoms of hebitol II (Taskova et al. 2011). Furthermore, the NMR data of **1** were highly similar to those of hebitol II, except for those of the p-hydroxyphenyl group in **1**, suggesting that the p-hydroxycinnamoyl group was attached to the C-6′ of glucopyranosyl and the C-6″ of mannitol moiety was attached to the C-1′. Subsequently, the linkage was confirmed by the HMBC correlations (Figure S2) of δ_H 4.52 and 4.29 (H-6′) with δ_C 169.1 (C-9), and of δ_H 4.36 (H-1′) with δ_C 73.7 (C-6″). The coupling constant of the anomeric proton (δ_H 4.36, d, $J=7.8$ Hz, H-1′) and the signal at δ_C 105.0 (C-1′) indicated the β-configuration of the glucose, and the absolute configuration of the sugar moieties were determined as *D*-glucose and *D*-mannitol by acid hydrolysis and GC analysis. Therefore, the new compound **1** was elucidated as 6-O-p-hydroxycinnamoyl-β-*D*-glucopyranosyl-(1→6)-*D*-mannitol, and named hebitol IV.

The other known compounds were identified as hebitol II (**2**) (Taskova et al. 2011), globularitol (**3**) (Caliş et al. 2002), syringin (**4**) (Venditti et al. 2017), 2-phenylethyl-β-D-glucopyranoside (**5**) (Liu et al. 2019), salidroside (**6**) (Yang et al. 2017), phenethyl alcohol-8-O-β-*D*-glucopyranosyl-(1→2)-β-*D*-glucopyranoside (**7**) (Ono et al. 1999), cistanoside F (**8**) (Kim et al. 2007), isocistanoside F (**9**) (Liu et al. 2016), verbascoside (**10**) (Li et al. 2013), isoverbascoside (**11**) (Li et al. 2013), campneoside II (**12**) (Kim et al. 2007),

isocampneoside II (**13**) (Kim et al. 2007), echinacoside (**14**) (Porter et al. 2015), angoroside A (**15**) (Li et al. 2011), forsythoside B (**16**) (Yamasaki et al. 2007), with their NMR spectroscopic data identical to those reported in the literature.

The compounds **1–16** were evaluated as potential VEGFR inhibitors by molecular docking and *in vitro* inhibitory activity assay. As shown in Table S2, the docking results showed that nearly half of the compounds were rated above 10.00 kcal/mol in absolute value, indicating their potential VEGFR-2 inhibitory activities. And a preliminary bioassay revealed that nine compounds (**7, 9-16**) exhibited inhibitory activity on VEGFR-2 at the concentration of 10 μM (the inhibition rate of each compound is over 50%). Further assay demonstrated that the compounds **10** and **14**, are potent natural inhibitors against VEGFR-2 with the IC_{50} values of 0.51 and 0.32 μM, respectively (Figure S3).

To investigate the potential retinal protective activity of **10** and **14**, BALB/c mice were administered with **10** or **14** at 100 mg/kg body weight (bw) 30 min before bright light exposure (10,000 lux for 30 min). Seven days after the bright light exposure, non-invasive optical coherence tomography (OCT) was employed to assess the changes of the retinal structure in a non-biased manner. As shown in Figure S6A and B, compared to the intact photoreceptor structure found in vehicle-treated mice without bright light exposure, bright light-exposed vehicle-treated mice exhibited severe impairment of photoreceptor structure, which was characterized by diminished outer nuclear layer (ONL). In contrast, well-preserved ONL and significantly increased thickness of ONL was observed in light-exposed mice treated with **10** or **14**. The results demonstrated remarkable photoreceptor protective activities of **10** and **14** *in vivo*.

3. Experimental

3.1. General experimental procedures

HR-ESI-MS were measured by an Agilent G6520 Q-TOF LC-MS spectrometer (Agilent Technologies Inc., Santa Clara, USA). Optical rotations were obtained on an Autopol VI 90079 polarimeter (Rudolph Research Analytical, Hackettstown, NJ, USA). IR spectra were recorded on a Thermo nicolet 6700 spectrophotometer (Thermo Fisher Scientific, MA, USA). UV spectra were measured on an Agilent 1260 infinity HPLC equipped with a DAD detector (Agilent Technologies Inc., Palo Alto, CA, USA). NMR spectra including ^{1}H NMR, ^{13}C NMR and 2 D NMR were recorded on a Bruker Avance III 600 spectrometer (Bruker Corporation, Rheinstetten, Switzerland), with chemical shifts referenced to tetramethylsilane (TMS) as an internal standard. GC analysis was carried out on a Shimadzu GCMS-QP2010E instrument (Shimadzu Corporation, Kyoto, Japan) equipped with a DB-5MS column (30 m × 0.25 mm × 0.25 μm). D-101 macroporous adsorption resin (Sinopharm Chemical Reagent Co., Ltd, Shanghai, China), Reversed-phase C18 silica gel (50 μm, YMC Co., Ltd, Kyoto, Japan) and Sephadex LH-20 (Pharmazia, Uppsala, Sweden) were used for column chromatography. TLC was performed on precoated silica gel plates (Yan Tai Zi Fu Chemical Group Co.; G60, F-254).

3.2. Plant material

The dried flowers and inflorescences of *B. officinalis* were purchased in 2018 from the market of Chinese herbal medicine in Bozhou, Anhui Province, China. The plants were identified by Dr. Yan-Hong Shi, Shanghai University of Traditional Chinese Medicine. A voucher specimen (No. MMH-20170427) was deposited in the Drug Discovery and Design Centre, Shanghai Institute of Materia Medica, Chinese Academy of Sciences.

3.3. Extraction and isolation

The air-dried flower buds of *B. officinalis* (10.2 kg) were reflux-extracted two times with distilled water (80 L) at 100 °C for 1 hour each time. The solution was combined and concentrated to 12 L, which was then partitioned with EtOAc and *n*-BuOH, successively. The *n*-BuOH fraction was subjected to column chromatography (CC) on a macroporous adsorption resin column, eluted with a gradient system of EtOH-H_2O (0:100 to 95:5) to yield four fractions (Fr.1-Fr.4). Fr.2 was chromatographed on a reversed-phase C_{18} silica gel (ODS) column and eluted with MeOH-H_2O (0:100 to 100:0) to give five fractions (Fr.2.1-Fr.2.5). Fr.2.1 was subjected to repeated CC on ODS columns eluted with MeOH-H_2O (0:10 to 3:7) and Sephadex LH-20 columns eluted with 10% MeOH to yield compounds **6** (53.7 mg). Fr.2.2 was separated on a Sephadex LH-20 column eluted with 5% MeOH to afford four subfractions (Fr.2.2.1-Fr.2.2.4). Fr.2.2.1 was purified subsequently by repeated CC on ODS columns eluted with MeOH-H_2O (0:10 to 3:7) and Sephadex LH-20 columns eluted with 10% MeOH, resulting in the isolation of compounds **1** (3.4 mg), **3** (9.5 mg), **4** (75.9 mg). Fr.2.2.2 was subjected to repeated CC on ODS columns eluted with MeOH-H_2O (0:10 to 3:7) and Sephadex LH-20 columns eluted with 10% MeOH to yield compounds **2** (4.3 mg), **8** (85.2 mg), **14** (719.0 mg), and **9** (12.7 mg). Compounds **10** (890.7 mg) were obtained from Fr.2.2.3 by CC on ODS eluted with MeOH-H_2O (0:10 to 3:7), and compound **12** (31.1 mg) was obtained from the further Sephadex LH-20 columns eluted with 10% MeOH. Fr.2.2.4 were purified by CC on ODS with a gradient of MeOH-H_2O (0:10 to 3:7) to afford compounds **13** (22.2 mg) and **11** (138.8 mg). Fr.2.3 was separated into six fractions (Fr.2.3.1-Fr.2.3.6) with the elution of MeOH-H_2O (0:10 to 6:4) on an ODS column. Fr.2.2.2 and Fr.2.2.5 was both subjected to repeated CC on Sephadex LH-20 columns eluted with 10% MeOH to give compounds **5** (30.1 mg), **7** (38.5 mg) from the former, together with **15** (6.1 mg), **16** (19.4 mg) from the latter.

3.3.1. Hebitol IV (1)

Yellowish amorphous power; [α]20D-10.6 (*c* 0.14, MeOH); IR (KBr) ν_{max} (cm^{-1}): 3355, 2923, 1695, 1630, 1603, 1586, 1514, 1437, 1261, 1169, 1073, 834, 525; UV (MeOH) λ_{max} (nm): 225, 310; HR-ESI-MS: *m/z* 513.1584 $[M+Na]^+$ (calcd for $C_{21}H_{30}O_{13}Na$, 513.1579). ^1H NMR (600 MHz, CD_3OD) δ_H: 7.64 (1H, d, $J=15.9$ Hz, H-7), 7.47 (2H, d, $J=8.6$ Hz, H-2, 6), 6.80 (2H, d, $J=8.6$ Hz, H-3, 5), 6.36 (1H, d, $J=15.9$ Hz, H-8), 4.52 (1H, dd, $J=11.9$, 2.0 Hz, H-6′a), 4.36 (1H, d, $J=7.8$ Hz, H-1′), 4.29 (1H, dd, $J=11.9$, 5.8 Hz, H-6′b), 4.16 (1H, dd, $J=10.5$, 2.4 Hz, H-6″a), 3.84 (1H, overlapped, H-4″), 3.81 (1H, overlapped, H-1″b), 3.79 (1H, overlapped, H-3″), 3.78 (1H, overlapped, H-5″), 3.72 (1H, dd, $J=10.5$, 6.2 Hz, H-6″b), 3.68 (1H, m, H-2″), 3.61 (1H, dd, $J=11.2$, 6.0 Hz, H-1″a), 3.55 (1H, m, H-

5′), 3.41 (1H, t, $J = 8.9$ Hz, H-3′), 3.37 (1H, overlapped, H-4′) , 3.27 (1H, dd, $J = 8.9$, 8.0 Hz, H-2′); ^{13}C NMR (150 MHz, CD_3OD) δ_C: 169.2 (C-9), 161.3 (C-4), 146.9 (C-7), 131.2 (C-2, 6), 127.2 (C-1), 116.8 (C-3, 5), 114.9 (C-8), 105.1 (C-1′), 77.7 (C-3′), 75.6 (C-5′), 75.2 (C-2′), 73.7 (C-6′′), 73.0 (C-2′′), 71.7 (C-5′′), 71.7 (C-4′), 71.2 (C-4′′), 71.0 (C-3′′), 65.2 (C-1′′), 64.6 (C-6′).

3.4. Determination of sugar components

The absolute configuration of sugars was determined by acid hydrolysis and GC analysis with the method described in the literature (Gao et al. 2017). Compound **1** (1 mg) was added in 2 mL 10% HCl/dioxane (1:1, v/v) and then heated at 80 °C for 2 h. After the reaction mixture was evaporated under N_2, the residue was dissolved in anh. pyridine (100 μL). Subsequently, 0.1 M L-cystein methyl ester hydrochloride (200 μL) was added, and the mixture was warmed for 1 h at 60 °C. Then, the 2.6 mL trimethylsilylation reagent HMDS-TMCS (hexamethyldisilazane/Me_3SiCl/pyridine, 2:1:10, v/v/v) was added, and warmed for 30 min at 60 °C. The mixture was partitioned with H_2O and cyclohexane (each for 2 mL), and the cyclohexane layer was analyzed by GC to identify the sugars. GC was conducted on the following conditions: cap. column, DB-5MS, (30 m × 0.25 mm × 0.25 μm); detection, FID; carrier, N_2 gas; detector and injection temp., 280 °C; initial temp. was maintained at 100 °C for 5 min and then raised to 280 °C at the rate of 35 °C/min, and final temp. was maintained for 9 min. As a result, the sugars were determined as *D*-mannitol (t_R = 11.45) and *D*-glucose (t_R = 14.48), with the retention times (t_R) of derivatives of the hydrolyzed **1** identical to those of authentic *D*-mannitol (t_R = 11.45) and *D*-glucose (t_R = 14.51) prepared in the same way as above.

3.5. Molecular docking study

Ensemble docking was performed for the identified compounds **1-16** against VEGFR-2. Firstly, all compounds were pre-processed by the Ligprep, with Epik to generate the proper protonation states at pH 7.0. Secondly, each ligand in ATP binding site of 26 VEGFR-2 structures (PDB IDs: 1y6b, 2oh4, 2p2h, 2p2i, 2qu5, 2qu6, 2rl5, 3b8q, 3b8r, 3be2, 3c7q, 3cp9, 3cpb, 3cpc, 3ewh, 3u6j, 3vhe, 3vhk, 3hng, 3vnt, 3vo3, 4ag8, 4agc, 4agd, 4asd, 4ase) was selected to define and generate the receptor grid. Thirdly, *in silico* docking of each compound against the 26 VEGFR-2 structures was performed by Glide in standard precision (SP) with default parameters. Fourthly, for each compound, the VEGFR-2 structure with the best docking score was chosen for further analysis. The docking modes of compounds **10** and **14** against VEGFR-2 are shown in Figure S4 and S5. All these computational calculations were performed in Schrödinger 2020 (Schrödinger LLC, New York, NY, USA).

3.6. Vegfr-2 inhibition assay

VEGFR-2(Cat#08-191, Carna) was diluted with enzyme buffer. The VEGFR-2 Kinase Assay Kit measures VEGFR-2 kinase activity for screening applications using HTRF

kinEASETM TK (Cat#62TKOPEC, Cisbio) as a detection reagent (Xu et al. 2020). The assay was carried out according to the supplied manual with modifications. The percentage of inhibition was calculated with the following equation: $(ER_{positive} - ER_{sample})/(ER_{positive} - ER_{negative}) \times 100\%$, where ER (emission ratio) is the ratio of 665 nm emission signal to 615 nm emission signal, and staurosporine was used as control. The 50% inhibitory concentration (IC_{50}) was obtained from the concentration-inhibition response curve ($n = 2$) comparing to staurosporine. Data were expressed as mean ± SD.

3.7. The potential retinal protective activity in vivo

3.7.1. Animals

BALB/c mice (4-5 weeks old) were obtained from Shanghai Laboratory Animal Research Center, China. Mice were maintained under a 12/12 h light/dark cycle with access to food and water at libitum. After dark adaption for 24 h, bright light exposure (compact fluorescence lamp, 45 W, Chaoya Lighting, Shanghai, China) was delivered at 10,000 lux for 30 min. **10** or **14** dissolved in H_2O was intraperitoneally administered to the mice 30 min prior to bright light exposure at 100 mg/kg bw ($n = 4$ per treatment). Mice unexposed to bright light ($n = 4$) and light-exposed mice ($n = 4$) without **10** and **14** treatment received H_2O vehicle treatment administered in the same manner. The animal care, handling and experimental protocols were reviewed and approved by the Institutional Animal Care and Use Committee of Yueyang Hospital, Shanghai University of TCM (Approval No. YYLAC-2019-021), which were carried out in adherence to the National Institutes of Health guide for the care and use of Laboratory animals (NIH Publications No. 8023, revised 1978).

3.7.2. Optical coherence tomography (OCT)

OCT (Micron IV, Phoenix Research Labs, USA) was carried out for *in vivo* imaging of mouse retina (Drexler and Fujimoto 2008). Ketamine hydrochloride (82.5 mg/kg bw) and xylazine (8.25 mg/kg bw) cocktail was intraperitoneally administered to the mice as anesthetics and the pupils were dilated by 1% tropicamide before OCT imaging. To quantify morphological changes, the OCT scans were subject to the measurement of the thickness of the outer nuclear layer (ONL) using Phoenix Reveal OCT software (Phoenix Research labs, USA). Data were expressed as mean ± standard deviation (SD). The statistical analyses were performed by one-way ANOVA. Statistical significance was defined by $P < 0.05$.

4. Conclusion

A new phenylethanoid, hebitol IV (**1**), along with fifteen known glycosides (**2**-**16**), were isolated from water extract of the flower buds of *Buddleja officinalis*. Their chemical structures were elucidated by MS, NMR spectrum data and comparisons with data reported in the literature. Among them, 9 compounds (**7**, **9**-**16**) showed VEGFR-2 inhibitory activities *in vitro*, and compounds **10** and **14** are potent natural inhibitors against VEGFR-2. Further assay *in vivo* demonstrated remarkable photoreceptor

protective activities of the compounds **10** and **14** in the mouse model featuring bright light-induced retinal degeneration.

Disclosure statement

No potential conflict of interest was reported by the authors.

Funding

This work was supported by the Natural Science Foundation of China (81603270, YZ; 81673790, YC), the Shanghai Sailing Program (16YF1414100), which are gratefully acknowledged.

ORCID

Zhijian Xu http://orcid.org/0000-0002-3063-8473

References

American Macular Degeneration Foundation. [date unknown]. Macular degeneration treatments. https://www.macular.org/treatments.

Caliş I, Kirmizibekmez H, Tasdemir D, Sticher O, Ireland CM. 2002. Sugar esters from *Globularia orientalis*. Z Naturforsch C J Biosci. 57(7–8):591–596. c:

Chinese Pharmacopoeia Commission. 2020. Pharmacopoeia of the People's Republic of China, vol. 1, Beijing: China Medical Science Press; p. 343.

Drexler W, Fujimoto JG. 2008. State-of-the-art retinal optical coherence tomography. Prog Retin Eye Res. 27(1):45–88.

Dugel PU, Koh A, Ogura Y, Jaffe GJ, Schmidt-Erfurth U, Brown DM, Gomes AV, Warburton J, Weichselberger A, Holz FG. 2020. HAWK and HARRIER: Phase 3, multicenter, randomized, double-Masked trials of brolucizumab for neovascular age-related macular degeneration. Ophthalmology. 127(1):72–84.

Editorial Committee of flora of China. 1992. Chinese Academy of Sciences, Flora of China, vol. 61. Beijing: Science Press; p. 277.

Gao YY, Zeng P, Jia CL, Zhang Y, Zhang T, Jia Q, Li YM. 2017. Two new phenols from *Lysimachia patungensis*. J Asian Nat Prod Res. 19(1):28–34.

Guo H, Koike K, Li W, Satou T, Guo D, Nikaido T. 2004. Saponins from the flower buds of *Buddleja officinalis*. J Nat Prod. 67(1):10–13.

Jie CH, Gao JS. 2004. Study of the effect of traditional Chinese herb butterflybush flower on the proliferation of vascular endothelial cells. Yanke. 13(6):348–350.

Kim JK, Si CL, Bae YS. 2007. Epimeric phenylpropanoid glycosides from inner bark of *Paulownia coreana* Uyeki. Holzforschung. 61(2):161–164.

Lee C, Lee S, Park SY. 2013. A New Monoterpene from the Flower Buds of *Buddleja officinalis*. Nat Prod Sci. 19(4):355–359.

Li HF, Peng QH, Yao XL, Wang F, Chen JW, Wu QL. 2009. Effects of *Buddleja offcinalis* flavone on dry eye syndrome and the expression of IL-1β, TNF-α in castrated rats. Guoji Yanke Zazhi. 9(7):1248–1251.

Li HM, Kim JK, Jang JM, Cui CB, Lim SS. 2013. Analysis of the inhibitory activity of *Abeliophyllum distichum* leaf constituents against aldose reductase by using high-speed counter current chromatography. Arch Pharm Res. 36(9):1104–1112.

Li L, Peng Y, Liu Y, Xu LJ, Guo N, Shi RB, Xiao PG. 2011. Two new phenethanol glycosides from *Ligustrum robustum*. Chin Chem Lett. 22(3):326–329.

Liu X, Li J, Li J, Liu Q, Xun M. 2019. A new flavonoid glycoside from *Ligularia fischeri*. Chem Nat Compd. 55(4):638–641.

Liu YF, Shi GR, Wang X, Zhang CL, Wang Y, Chen RY, Yu DQ. 2016. Chemical constituents from whole plants of *Rehmannia chingii*. Zhongcaoyao. 47(11):1830–1833.

Matsuda H, Cai H, Kubo M, Tosa H, Iinuma M. 1995. Study on anti-cataract drugs from natural sources. II. Effects of buddlejae flos on *in vitro* aldose reductase activity. Biol Pharm Bull. 18(3):463–466.

Ono M, Yoshida A, Ito Y, Nohara T. 1999. Phenethyl alcohol glycosides and isopentenol glycoside from fruit of *Bupleurum falcatum*. Phytochemistry. 51(6):819–823.

Park TW, Lee C, Lee JW, Jang H, Jin Q, Lee MK, Hwang BY. 2016. Chemical constituents from *Buddleja officinalis* and their inhibitory effects on nitric oxide production. Nat Prod Sci. 22(2): 129–133.

Porter EA, Kite GC, Veitch NC, Geoghegan IA, Larsson S, Simmonds MSJ. 2015. Phenylethanoid glycosides in tepals of *Magnolia salicifolia* and their occurrence in flowers of Magnoliaceae. Phytochemistry. 117:185–193.

Shen ZH, Zuo ZQ, Liu J. 2016. Effect of Chinese medicine Flos Buddlejae on vascular endothelial growth factor of corneal neovascularization in alkali-burned mice. China J Chin Ophthalmol. 26(3):161–165.

Sheng GQ, Zhang JR, Pu XP, Ma J, Li CL. 2002. Protective effect of verbascoside on 1-methyl-4-phenylpyridinium ion-induced neurotoxicity in PC12 cells. Eur J Pharmacol. 451(2):119–124.

Tai BH, Jung BY, Cuong NM, Linh PT, Tung NH, Nhiem NX, Huong TT, Anh NT, Kim JA, Kim SK, et al. 2009. Total peroxynitrite scavenging capacity of phenylethanoid and flavonoid glycosides from the flowers of *Buddleja officinalis*. Biol Pharm Bull. 32(12):1952–1956.

Tai BH, Nhiem NX, Quang TH, Ngan NT, Tung NH, Kim Y, Lee JJ, Myung CS, Cuong NM, Kim YH. 2011. A new iridoid and effect on the rat aortic vascular smooth muscle cell proliferation of isolated compounds from *Buddleja officinalis*. Bioorg Med Chem Lett. 21(11):3462–3466.

Taskova RM, Kokubun T, Ryan KG, Garnock-Jones PJ, Jensen SR. 2011. Iridoid and phenylethanoid glucosides from *Veronica lavaudiana*. J Nat Prod. 74(6):1477–1483.

Venditti A, Sanna C, Lorenzetti LM, Ballero M, Bianco A. 2017. New coumarinyl ethers in *Daphne oleoides* Schreb. collected from Sardinia Island. Chem Biodiversity. 14(6):e1700072.

World Health Organization. 2021. Blindness and vision impairment. https://www.who.int/en/news-room/fact-sheets/detail/blindness-and-visual-impairment.

Xie G, Xu Q, Li R, Shi L, Han Y, Zhu Y, Wu G, Qin M. 2019. Chemical profiles and quality evaluation of *Buddleja officinalis* flowers by HPLC-DAD and HPLC-Q-TOF-MS/MS. J Pharm Biomed Anal. 164:283–295.

Xu HC, Wang MS, Wu FX, Zhuo LS, Huang W, She NF. 2020. Discovery of N-substituted-3-phenyl-1,6-naphthyridinone derivatives bearing quinoline moiety as selective type II c-Met kinase inhibitors against VEGFR-2. Bioorg Med Chem. 28(12):115555.

Yamasaki T, Masuoka C, Nohara T, Ono M. 2007. A new phenylethanoid glycoside from the fruits of *Callicarpa japonica* Thunb. var. *luxurians* Rehd. J Nat Med. 61(3):318–322.

Yang Y, Yang YB, Lu WQ, Wu ZJ, Chen WS. 2017. A new hydroxyjasmonic acid derivative from *Polygonum capitatum*. Chem Nat Compd. 53(3):417–421.

Zhang HY, Pan JX. 1996. Phenylpropanoid glycosides and flavonoid glycosides isolated from buds of *Buddleja officinalis* Maxim. J Chin Pharm Sci. 5(2):105–110.